PERCOLATION BEHAVIOR IN THE Fe-Ni-Si-S-C SYSTEM AND INFLUENCE ON METEORITE COMPOSITIONS

A. Lindoo[1], M. S. Duncan[1], and Y. Fei[1], [1]Geophysical Laboratory, Carnegie Institution for Science, Washington, D.C., USA (alindoo@carnegiescience.edu)

Introduction: Meteorites provide a "window" into planetary interiors; allowing us to better understand evolution of the early solar system and planetary differentiation. Iron meteorites in particular present a unique opportunity to study core formation processes. The variety in chemical compositions between iron meteorite groups points to complex accretion and differentiation histories of their parent bodies. Understanding core-mantle segregation processes under different accretionary conditions can provide insight into the range of chemical compositions recorded in meteorites.

Two mechanisms are often cited to describe metal segregation and core formation: (1) the existence of a magma ocean and (2) metallic melt percolation through a solid silicate matrix [1]. Planets may experience different segregation processes depending on heat source and thermal evolution, but differentiation via percolation is likely the dominant process for smaller planetary bodies when heated to temperatures high enough to melt the metallic component [2]. Metallic melt migration through a porous matrix is primarily controlled by melt volume and the chemical composition [3–5]; the latter most notably affects the wettability of the liquid. Iron meteorites, dominantly composed of Fe and Ni, also contain small amounts of light elements including sulfur, silicon, carbon, and phosphorous [6]. Light elements have proven to reduce melt/olivine interfacial energy, though show a range in this effect. For example the addition of sulfur or oxygen reduces the dihedral angle while silicon has no effect [1,7–11]. However, studies to date have largely determined percolation behavior for binary or ternary systems via dihedral angle measurements.

Our objective is to better understand the physical process of percolation in a complex system of multiple light elements. Our experiments address the following questions: (1) What are the compositions of the immiscible liquids in the Fe-Ni-Si-S-C system? (2) What is the percolation behavior of the immiscible liquids (i.e., can the two phases physically separate during transport through cracks/grain boundaries)? (3) How does temperature affect percolation behavior, especially when partial melting of metal occurs? (4) Can we relate composition evolution during percolation to meteorite compositions?

Methods: To simulate liquid metal percolation in a small planetary interior, we performed piston-cylinder experiments at temperatures between 1100–1600 °C at 1 GPa. Two compositions were employed to observe the effects of light elements on percolation behavior: Fe + 5 wt.% Ni + 6 wt.% Si + 2 wt.% S and Fe + 5 wt.% Ni + 2 wt.% Si + 6 wt.% S. Powders were loaded into graphite capsules to allow C saturation in the experiments (≤ 6.4 wt.%). Within the graphite capsule, we used two capsule configurations: (1) San Carlos (SC) olivine inner "capsule", where powdered SC olivine fully surrounded the metal sample or (2) a SC olivine-metal-SC olivine "sandwich". The capsule along with MgO spacers was placed within a half inch talc-pyrex assembly with graphite heaters. Samples were pressurized to 1 GPa and heated to 800 °C and sintered for two hours. The experiments were then heated to the target temperatures and held for 3–12 hours before quenching. The experimental products were polished and their chemical compositions analyzed with the electron microprobe (EMP). Apparent dihedral angles were measured on 2D images captured during EMP analysis or with the scanning electron microscope (SEM).

Results: Both starting compositions form immiscible Fe-Ni-S and Fe-Ni-C liquids (Fig. 1) that coexist with a solid Fe-Ni-Si-C alloy at lower experimental temperatures. The Fe-Ni-S melt wets the surrounding olivine grains and carries the non-wetting, C-rich Fe-Ni alloy into the olivine matrix. The C-rich melt is always found suspended within the Fe-Ni-S melt and shows no evidence of segregation from the wetting phase (Fig. 2).

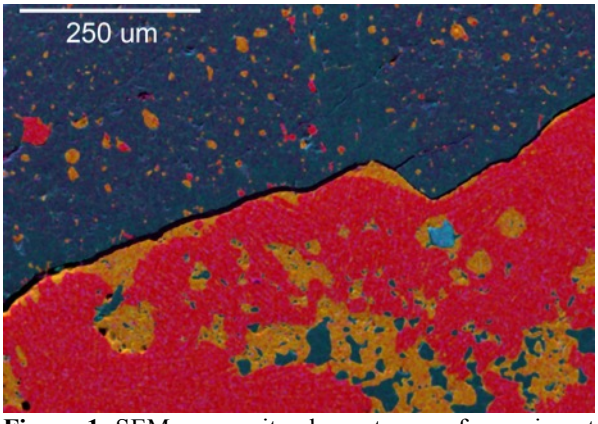

Figure 1. SEM composite element map of experiment PC1674b, 1500 °C at 1 GPa. Fe-Ni-S melt (yellow) transports a C-rich Fe-Ni melt into the surrounding olivine matrix (blue). A Fe-Ni-Si-C melt (red) remains in the initial loading area along with residual Fe-Ni-S melt.

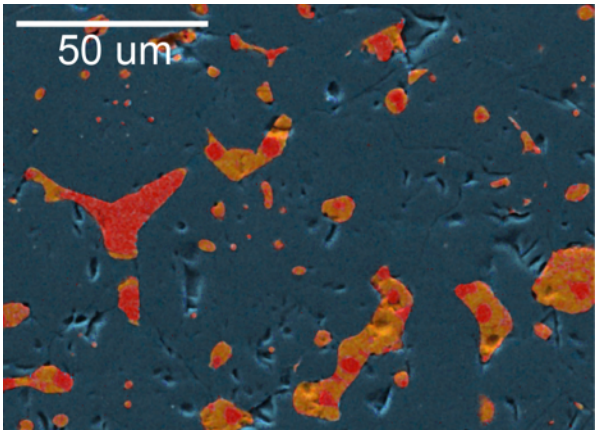

Figure 2. Zoomed in section of PC1674b SEM composite element map (T = 1500 °C, P = 1 GPa) illustrating percolation texture of immiscible Fe-Ni-S melt (yellow) and C-rich Fe Ni alloy (red) within San Carlos olivine grains (blue).

The average apparent dihedral angle of the Fe-Ni-S melt is ~80° and does not appear to change with increasing temperatures (less Ni in melt). In experiments with lower S concentrations (2 wt.%), the majority of the Fe-Ni-S melt is found in the olivine matrix. However, not all of the Fe-Ni-S melt percolates into the olivine in experiments utilizing the higher S starting composition (6 wt.%). Instead, a fraction of melt remains with the Fe-Ni-Si-C alloy in the initial loading region. The Fe-Ni-Si-C alloy never percolates into the olivine, even when fully molten.

Discussion: Immiscible Fe-Ni-S and Fe-Ni-C melts percolate soon after the system reaches the eutectic temperature. Because of rapid percolation following melting, it is unlikely that the immiscible liquids would remain in equilibrium with the Fe-Ni-Si-C alloy. Similar to previous studies, the Fe-Ni-S melts controls percolation through the silicate matrix [11–13]. In all experiments, the C-rich liquid is found surrounded by the Fe-Ni-S melt and shows no examples of physical separation. Higher temperatures do not change the measured dihedral angle, indicating that the presence of sulfur in the Fe-Ni-S melt is largely responsible for lowering interfacial energy.

The efficiency of percolation depends on the percolation threshold defined by the volume fraction of metal and the dihedral angle determined by the interfacial energies of the solid-solid and solid-liquid interfaces. Despite the dihedral angle of the Fe-Ni-S melt being higher than the critical angle determined for melt connectivity, percolation still occurs. The melt percolation along the stagnant Fe-Ni-Si-C alloy may reflect high melt percentage as melting proceeds. The observed percolation behavior could lead to S distributions in silicate and metal alloy that are not purely governed by equilibrium process, providing a potential explanation for variations in bulk S concentrations in iron meteorites. The percolation of a Fe-S melt away from the stagnant Fe-Ni alloy during melting may explain the absence of S noted in the meteorite record, most notably the IIAB irons [6].

Silicon is found primarily within the immobile alloy in our experiments. Silicon partitioning between metal and silicate is strongly controlled by the oxygen fugacity, therefore high Si content in the metallic alloy generally reflects a highly reduced environment. Few iron meteorites contain appreciable amounts of Si. Indeed, concentrations are consistently much lower than expected under metal-silicate equilibrium conditions [14]. Very low Si concentrations in iron meteorites are at odds with some of the highly reduced accretion models. Our experimental results would imply that most iron meteorite parent bodies were not differentiated in highly reduced environments.

References: [1] Shannon M. C. and Agee C. (1998) *Sci., 280*, 1059–1061. [2] Kleine et al. (2002) *Nature, 418*, 952–955. [3] von Bargen N. and Waff H. S. (1986) *JGR, 91*, 9261–76. [4] Minarik W. G. et al. (1996) *Sci., 272*, 530– 533. [5] Yoshino et al. (2003) *Nature, 422*, 154–157. [6] Benedix G. et al. (2013) *in Treat. Geochem., 2*, 267–285. [7] Shannon M. C. and Agee C. (1996) *GRL, 23*, 2717–2720. [8] Terasaki H. et al. (2005) *EPSL, 232*, 379–392. [9] Mann U. et al. (2008) *PEPI, 167*, 1–7. [10] Holzheid A. et al. (2013) *EJM, 25*, 267–277. [11] Duncan M. S. and Fei Y. (2017) *LPS XLVIII*, Abstract #1505. [12] Corgne A. et al. (2008) *GCA, 72*, 2409–2416. [13] Fei Y. and Shibazaki Y. (2016) *LPS XLVII*, Abstract #1719. [14] Pack A. et al. (2011) *MaPS, 10*, 1470–1483.